Available online at www.sciencedirect.com

ScienceDirect

Procedia Engineering 130 (2015) 701 – 710

Procedia Engineering

www.elsevier.com/locate/procedia

14th International Conference on Pressure Vessel Technology

Microstructure Characteristics of 12Cr1MoV Heat Pipes with the Combined Effects of Compression Creep and Molten Alkali Salts Corrosion

W.Z. Xiong[a,*], J.J. He[a], J. Chen[a], K.L. Long[a], Z.H. Zheng[a]

[a]*School of Energy and Power Engineering, Changsha University of Science and Technology, 960, 2nd Section, Wanjiali South RD, Changsha, Hunan, 410004, P.R.China*

Abstract

12Cr1MoV is one of the low alloy steels which is widely applied in heat pipes of biomass fired boilers. But with the combined effects of molten alkali salts corrosion caused from combustion of biomass and creep deformation which is resulted by the high temperature stress as well as steam pressure, they bring negative influence on the mechanical properties. Based on the fact, the present work mainly focuses on studying the microstructure deformation of samples after compression creep in different molten alkali salts. 12Cr1MoV steels chosen as candidate materials are first cut by EDM. Molten salts conditions are described as NaCl-40%KCl, NaCl-70%KCl and NaCl-40%Na_2SO_4. Creep properties of 12Cr1MoV in molten salts were obtained by the creep test at 150MPa. Experiments were tested on RDL05 electronic creep fatigue test machine after reformation to create a condition of hot corrosion. The results showed that different creep deformation was generated by different salt mixtures. When the temperature was set at 650℃, sample in molten NaCl-70%KCl showed the severest destruction than other samples on surfaces and cross sections. In these areas, the applied stress played a synergic role with corrosion leading to the progressive loss of material load-bearing capacity. On the substrate, spheroidization of cementites and precipitation of carbides along grain boundaries were clearly detected, which is also the reason to lower the strength of 12Cr1MoV. It is interesting to note that creep deformation of microstructures in NaCl-40%Na_2SO_4 was the weakest, indicating that sulfates can suppress corrosion effects of molten chlorides.

Peer-review under responsibility of the organizing committee of ICPVT-14

Keywords: Heat pipes, 12Cr1MoV, Molten alkali salts corrosion, Microstructure, Compression creep.

* Corresponding author. Tel: +86 731 85258408; Fax: +86 731 85258409.
E-mail address: ansonhiong@126.com

Peer-review under responsibility of the organizing committee of ICPVT-14
doi:10.1016/j.proeng.2015.12.166

1. Introduction

The iron-base low alloy steel, 12Cr1MoV is one of the most utilized high temperature material components widely applied as heat pipes materials in biomass fired power plant. The relative low percent volume of alloying elements makes the steel more economical. The good strength, toughness and ductility can be improved with the character of solution strengthening and dispersion strengthening caused by elements in matrix [1-2]. It has further been proved that the steel has a relative high heat conductivity and good heat resistance which enables the material to operate at high temperature for long duration [3].

As a renewable energy source, the biomass fuel and its utilization are gaining an increasingly important role worldwide. However, biomass fuels with high concentrations of Na, K, Cl and S are usually used for firing industrial processes. During the combustion of these products, alkali metal salts with low melting points will combine with other ash constituents and deposit on cooler component surfaces [4]. The molten salts will interact with substrate elements (Fe, Cr, Mn), resulting in sever corrosion caused by oxidation and hot corrosion, both of which have serious effects on the safe performance of materials [5-8]. At the same time, heat pipes can be deformed by the high temperature stress and steam pressure. With the appearance of stress, volume expansion caused by corrosion products is attacked along grain boundaries. Cracks in these areas are formed and expanded when steels were exposed in high temperature for a long time [9-12]. In the long-term operation of pipes at high temperature, the damage and protection due to corrosion and creep behavior have been taken into consideration in recent researches. In the study of corrosion, it had been reported that molten NaCl generates sever corrosion as well as internal void formation of steels while the feature of intergranular attack is more pronounced as the content of Na_2SO_4 in the mixtures[4]. Van lith et al. studied corrosion in biomass combustion and showed that KCl increase the corrosion rates of materials which is used as super heater tubes [13]. For the reason that the presence of chlorides has allowed a salt phase to exist at the metal scale interface and supported a higher concentration of dissolved Cr and Fe, some investigations have proved that the mixed chlorides argue for a fast corrosion rate [14-16]. From creep researches of alloys, macro-aspect methods which explained mechanism of deformation were studied [17-19]. However, high temperature creep behaviors can be better explained by studies at micro-aspect level. For example, O.Prat et al. [20] indicated that the precipitate of laves phase is an important intermetallic precipitate that significantly influenced microstructures as well as mechanical properties in 9-12% Cr steels. Meanwhile, some important conclusions about the combined effects of molten salts and load stress have been made. Lin D.L. [21] has proved that the creep rupture life and ductility of the salt-coated specimens are reduced dramatically, but the salt corrosion dose not change the creep mechanism. S.Bagui et al. [22] noted that salt mixture affects the creep rupture properties of the material catastrophically only after certain period of time.

The creep properties of salt-coated alloy are available in literature. Most studies mainly focuses on the influence of single saline environment on creep rupture life[21], deformation mechanisms of alloy and tensile creep properties[21-23]. However, data of creep properties of 9-12% Cr steels in various molten salts conditions is still not available because different salts have different degree of severity to corrode. Meanwhile, researches of compression creep of steels are not widely reported. For the complicated working environment of alloys, not only the tensile stress but also the compression stress should be both considered. Therefore, the objective of this study is to explain the compression creep behaviors of 12Cr1MoV in different molten alkali salt environments. Since the corrosion in working environment is continuous, the salt-coatings on creep specimen from traditional studies are replaced by a container full of salts where the sample can be wholly immersed and the salts mixtures will not easily evaporate in high temperature. Creep tests in corrosion condition were carried out at the load stress of 150MPa to achieve creep curves. The detailed microstructure of corrosion surface, section areas and substrate were observed by scanning electron microscopy (SEM) with energy dispersive spectroscopy (EDS). Relationships between creep and corrosion behaviors and microstructures were detailed analyzed.

2. Experimental process

The heat-treated 12Cr1Mo1V heat pipes steel was chosen as the raw material in this experiment, the chemical components are shown in Table.1. Creep specimens were prepared by cutting 16mm height, 9mm diameter cylindrical rods from raw materials by EDM.

Specimens using for creep test were made on RDL05 electronic creep fatigue test machine after reformation. A container where molten alkali salts were filled was designed under the indenter, as shown in Fig.1. All the devices were exposed to the air condition. The range of extensometer is 25mm and the deformation measurement range is 5 mm. The gauge area of sample was polished to obtain a smooth surface. Heat preservation of ingots was set as 30min before experiments to make specimens under uniform heating. Compression creep curves were obtained with load stress of 150Mpa.

Table 1. Chemical compositions of 12Cr1MoV steels.

C	Si	Cr	Mn	Mo	V
0.08～0.15	0.17～0.37	0.90～1.20	0.40～0.70	0.25～0.35	0.15～0.30

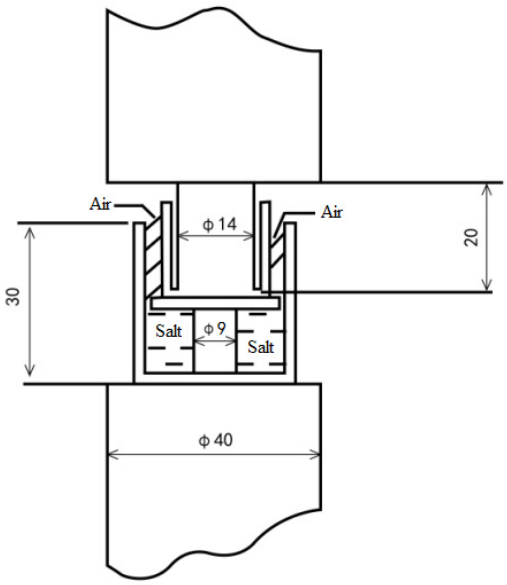

Fig. 1. Compression creep devices after reformation.

3. Results and discussion

3.1. Creep curves

Figure2 shows the relationship between the true specimen strain and time (creep curves) of 12Cr1MoV in different molten salt conditions at the stress of 150MPa. It can be seen from Fig.2 that different creep rates of specimens were resulted in different molten salt conditions. The sample in molten NaCl-40%Na_2SO_4 expose the lowest creep rate and the compression creep strain of which is nearly about 0.018. When Na_2SO_4 are taken place by KCl in the same mass ratio, creep become more obvious and the creep strain is approximately near 0.022. It can be clearly observed from the curve that the creep rate shows a maximum value of three samples when in the molten NaCl-70%KCl. The compression creep strain is nearly two times of other specimens. All results obviously indicating that the strength and plasticity of corrosion products are different with various reactions of molten salts, which seriously affect creep properties of materials. It has been concluded that creep deformation generated by molten chloride mixtures is much stronger than molten NaCl-40%Na_2SO_4 and the effects are also aggravated by the increase of KCl.

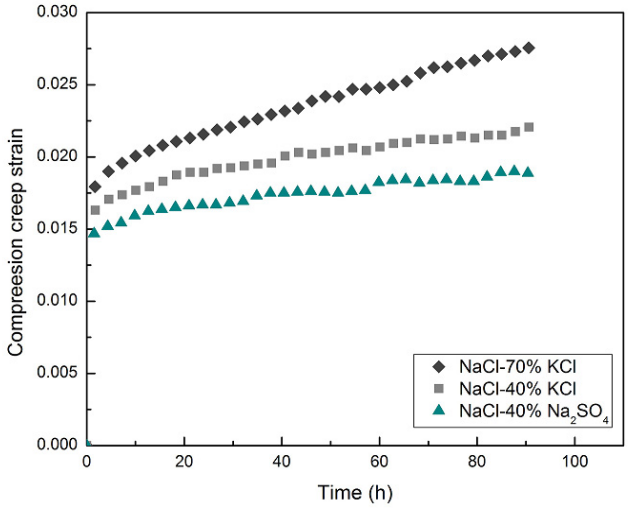

Fig. 2. Creep curves of 12Cr1MoV in alkali molten salts under the stress of 150MPa.

3.2. Microstructure of corrosion surface

Through the further experimental study, there is a necessity to analysis the microstructure details in different parts of materials. Fig.3 shows corrosion surface and EDS spectra in different molten mixtures. Fig.3(a) is the corrosion surface resulted by NaCl-40%KCl after creep deformation. The failure mechanisms on the surface can be defined as intergranular corrosion. Grain boundaries were clearly observed, which were covered by granular corrosion products. Meanwhile, some small bright spots are distributed near those products. The spots are inferred as mixtures of KCl and NaCl salts for the reason that abundant Cl was detected by EDS detection (spectra.1). According to the atomic percentage of Fe and O, oxide products are examined as Fe_2O_3. As shown in Fig.3 (b), an evident difference on the corrosion surface could be observed with the increase of KCl. The oxide films are totally spalled off with loose and porous morphology. Numbers of cracks and defected structures were observed on the products. According to the EDS analysis in spectra.2, abundant O were detected, which shows that the surface is extremely corroded by molten salts. The content of O is much higher than in spectra.1, indicating that the corrosion in molten NaCl-70%KCl is stronger.

Previous effects are resulted by the *active oxidation of chlorine* and load stress [24]. Reactions are shown in Eq.1-Eq.3. Corrosion mixtures with high oxygen value and low melting point are produced because of the reaction between molten NaCl-KCl and Fe, Cr in substrate. Besides, Cl_2 is also generated in the reaction. In a next step, if Cl_2 penetrates the oxide scale through pores or cracks, metal chlorides are able to form at the substrate. A number of pores occur on the surface when the low-melting metal chlorides break through oxide films. These holes will destruct the completeness of whole surface leading to the appearance of bubbles, uplifts and ruptures.

$$2NaCl + Fe_2O_3 + 1/2O_2 \rightarrow Na_2Fe_2O_4 + Cl_2 \quad (1)$$

$$M + 1/2Cl_2 \rightarrow MCl \quad (2)$$

$$2FeCl_2 + 3/2O_2 \rightarrow Fe_2O_3 + 2Cl_2 \quad (3)$$

When there is a load stress on the sample, pores are squeezed and expanded to be cracks and fault structures, which accelerate the destruction and exfoliation of oxide films. From Fig.3(c), long slab-like products without

obvious cracks and pores were observed on the sample in molten NaCl-40%Na_2SO_4, The morphology of which is totally different from Fig.3 (a) and Fig.3 (b). From the EDS detection, abundant Fe and O were detected. At the same time, Cr and S also exist on the corrosion products. The main corrosion mechanism by molten sulfate is described in Eq.4:

$$Fe_2O_3 + 3SO_3 \rightarrow Fe_2(SO_4)_3 \quad (4)$$

In this equation, gaseous SO_3 is generated by the molten sulfate in high temperature condition. The oxide film of materials is attacked by the complicated combination and decomposition reactions. Compared with the corrosion of chloride, the corrosion caused by sulfate is much slighter because active oxidation will not be formed during this reaction. At the same time, the generated sulfate mixtures are stable on which concentrated defected structures were not observed. The compact products can lead to a relative protection on the strength of material, where creep is not as obvious as in molten chloride mixtures.

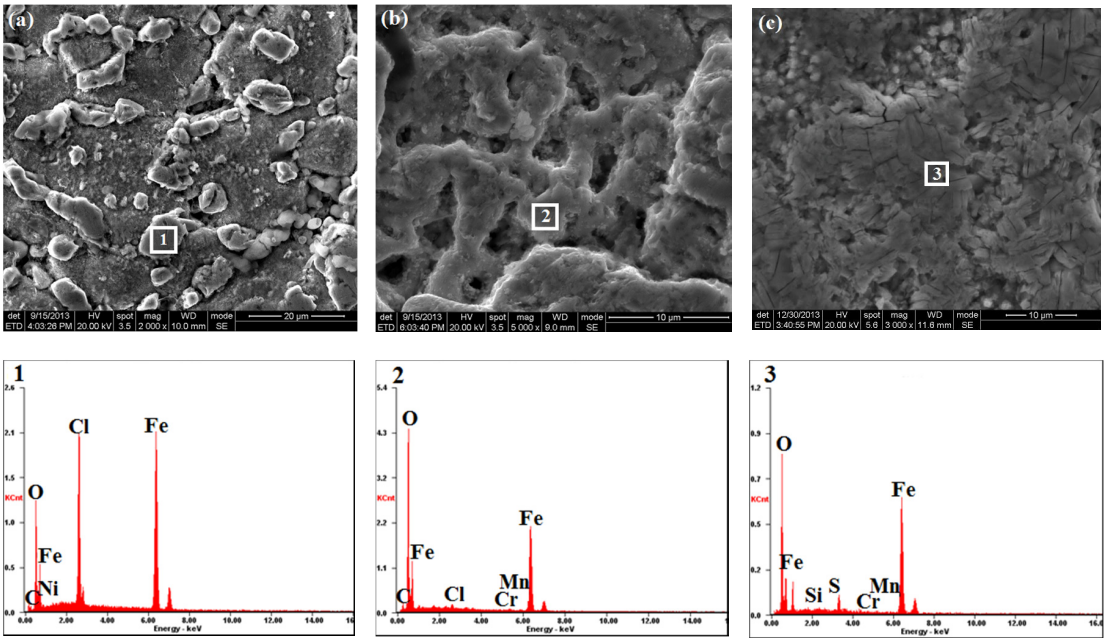

Fig. 3. Microstructure of the corrosion surface in molten (a) NaCl-40%KCl; (b) NaCl-70%KCl; (c) NaCl-40%Na_2SO_4 under the stress of 150MPa with EDS analysis.

3.3. Microstructure of section areas

Figure 4 reveals microstructure characteristics of cross sections where corrosion depth and internal attack can be reflected with different molten salt environments at 650℃. The load stress is set as 150MPa. Fig.4 (a) shows the morphology of the cross section in molten NaCl-40%KCl. According to the EDS, layers with different contents of O and Cl were observed in this area, indicating that corrosion strength by molten salts is weakened with the increasing depth of corrosion. The obvious cracks are caused by the combined effects of load stress and internal corrosion where the load stress can aggravate the separation between the layer and substrate. With the increase of KCl as shown in Fig.4 (b), evident cracks are also formed on cross secion. However, pores with large size were observed, which are not showed in Fig.4 (a). From EDS identification, Fe, O and Cl were all detected in corrosion layer (spectra.2) and substrate (spectra.1), indicating that the corrosion is strong in NaCl-70%KCl. Fig.4 (c) shows the section area of the sample in NaCl-40%Na_2SO_4. The corrosion layer is much thicker than the layer in other salts and

abundant Fe, Cr, O and S without Cl were detected on the layer by EDS (spectra.2). This can be explained that the existence of sulfate suppress corrosion effects of chlorine. At the same time, active oxidation of sulphur is not happening, which also weaken the growth of pores and inclusions. When compared with the sample in molten chloride mixtures, obvious cracks will not be generated. Results better illustrate that the corrosion effects generated by NaCl-40%Na_2SO_4 is much slighter than in molten chloride mixtures. It can be concluded from figures that creep deformation in cross section is seriously affected by the species of salts. Cracks can be generated in molten chlorides when there is a appropriate stress on the sample. Meanwhile, the amount of cracks increases with the increase of KCl. When compared with Fig. 4(a) and Fig.4(b), the corrosion layer in NaCl-70%KCl is different from which in NaCl-40%KCl. Many defected structures such as pores with large sizes and inclusions were observed. This is because when the sample is exposed in corrosive medium, the molten salts will interact with alloy elements when permeating into the layer and substrate. The expanding of corrosive products after reaction will defects complex inclusions and cells [25]. Effects of adhesion among grains are weakened by molten salts corrosion. At the same time, glide caused by compression creep also accelerates the destruction of adhesion. Stress concentration can be easily raised in those defected structures, inducing the distortion and fracture failures of 12Cr1MoV on the corrosion layer. Numbers of small holes in substrate of both samples can be explained as the result of active oxidation, which has been discussed before. The permeation of Cl_2 generated by the oxidation of metal chlorides can break through the substrate and make the appearance of holes. From the change of cross section, in conclusion, the applied stress plays a synergic role with corrosion, leading to the progressive loss of material load-bearing capacity.

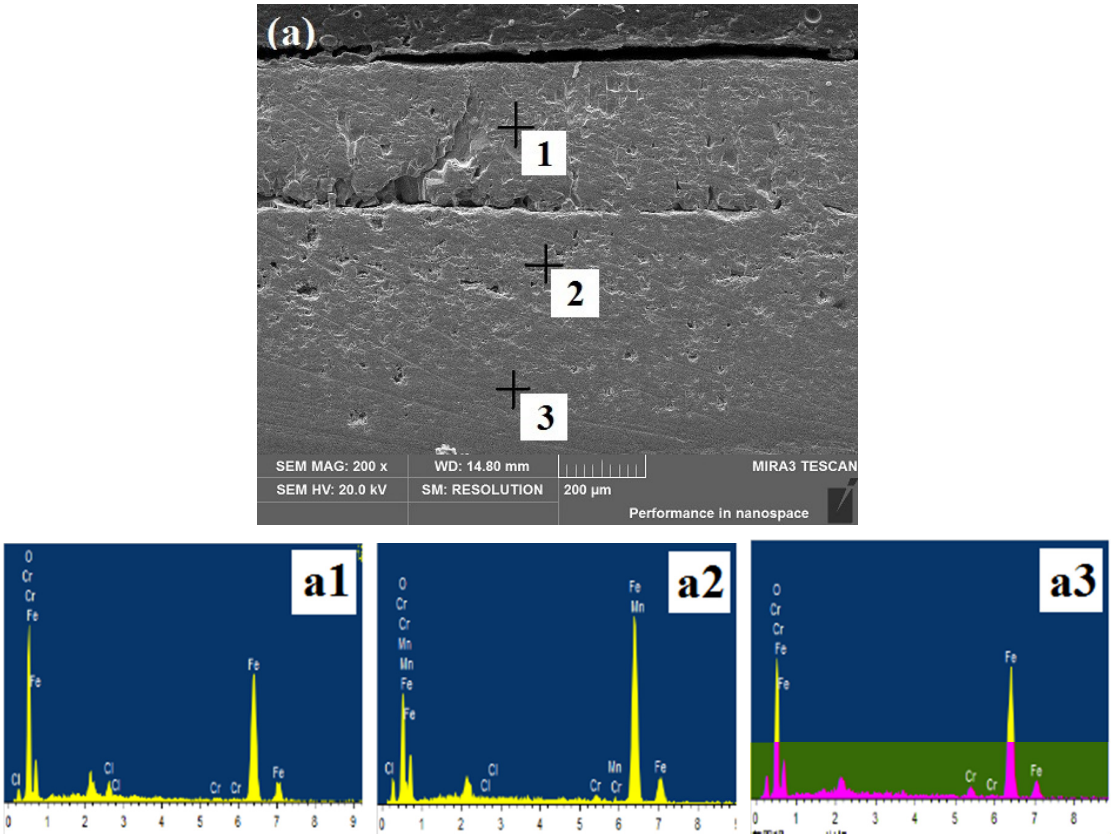

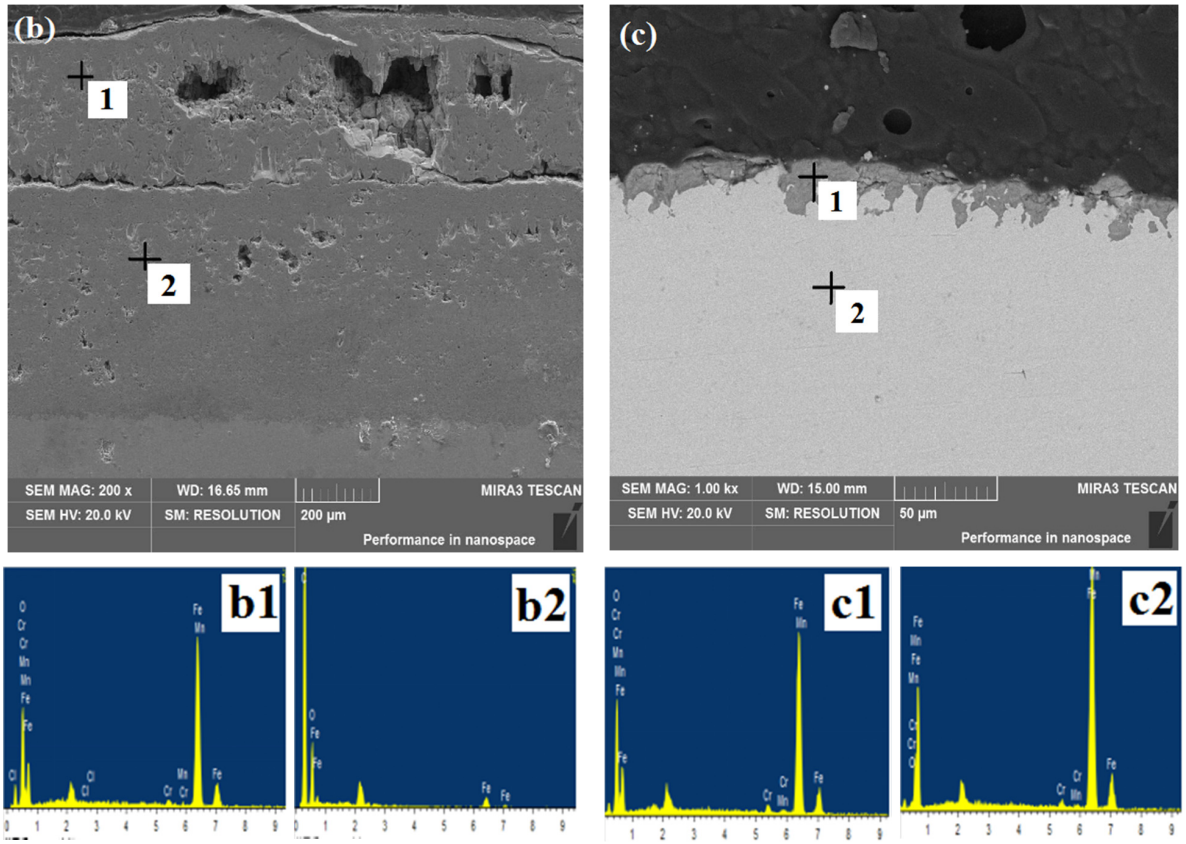

Fig. 4. Microstructure and EDS spectra of the corrosion section in molten (a) NaCl-40%KCl; (b) NaCl-70%KCl; (c) NaCl-40%Na_2SO_4 under the stress of 150MPa.

3.4. Microstructure of substrate areas

The appearance of the specimens in substrate after compression was observed by SEM. Grains and grain boundaries display different structures in different experimental environment as shown in Fig.4. In 650℃ molten chlorides, the microstructure as shown in Fig.5 (a)-(b) exposes squeezed grains and evident grain boundaries during the high temperature creep deformation. The compression of grains in Fig.5 (b) is more severe than in Fig.5 (a), which again proves that the sample in molten NaCl-70%KCl is easier to be deformed. The coarse grain boundaries are caused by the glide of grains. Pearlites in both samples are exposed as small pieces, which are divided by the load stress. Fig.5(c) displays the microstructure of the specimen in molten NaCl-40%Na_2SO_4. Slightly squeezed grains and grain boundaries were observed and pearlites expose large-flake morphology which is not totally divided into several pieces.

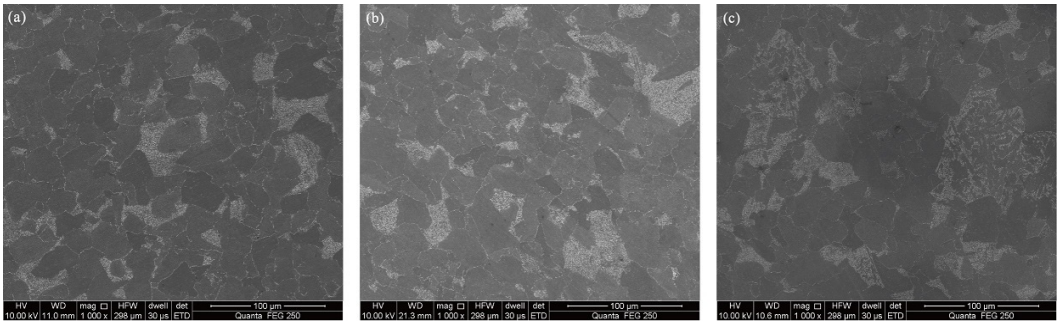

Fig. 5. Microstructure of the substrate in molten (a) NaCl-40%KCl; (b) NaCl-70%KCl; (c) NaCl-40%Na_2SO_4 under the stress of 150MPa.

To analysis specific change of microstructure in substrate, the morphology of substrate in molten salts after further amplification were observed. For the reason that the morphology of precipitated carbides, pearlites and eutectoid cementites are nearly the same in different molten salts, but there exist an obvious difference between the as-received sample and samples after creep deformation in molten salts, Fig.6 shows a comparison of substrate microstructure of the as-received sample and sample in molten NaCl-70%KCl. When comparing with the as-received sample, many coarse grain boundaries were observed surrounding the pearlite which indicates that the grains were under compression for a long time where the grain boundary sliding happens. Meanwhile, numbers of precipitated carbides were observed along grain boundaries in Fig.6 (b).

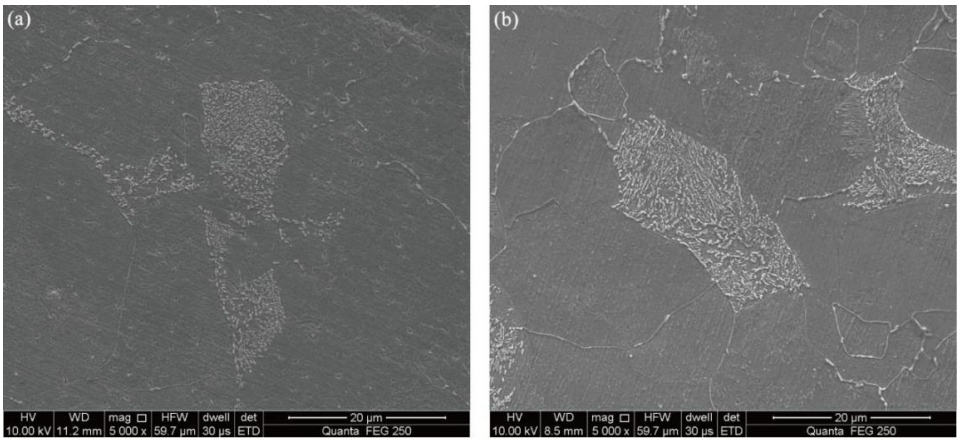

Fig. 6. Microstructure of the substrate (a) as-received sample; (b) sample in molten NaCl-70%KCl under the stress of 150MPa.

The elements of precipitated carbides were identified by EDS in Fig. 7(a). Results shows that iron (Fe) and carbon (C) with the atomic mass percentage of 77.21% of Fe, and 19.97% of C are main elements and there exist a small number of chromium (Cr), inferred that the precipitates on grain boundaries is similar to Fe_3C (tertiary cementite). With a complex spacing structure, the carbides only precipitate out in extreme conditions. Grain boundary embrittlement is aroused when tertiary cementite distribute on grain boundaries. Comprehensive mechanical properties can be weakened by excessive precipitates, resulting the softening and deformation of in substrate of 12Cr1MoV steels. The evident corrosion pit around those precipitates in this figure is caused by the molten salts mixtures. When there is a stress on the sample, the corrosion generated by molten salts is heterogeneous, which result the deep corrosive depth in some area. Fig.7 (b) shows the microstructure of eutectoid cementites of the sample. Some cementites were observed as arborization while parts of which are exposed as spot-like structure. The phenomenon is described as the spheroidization of cementites which can lower the yield point, creep strength, creep

limit and creep modulus of 12Cr1MoV steels, resulting in a bad influence on the property of material [26]. As the corrosion in different molten mixtures hardly affected substrate areas, the precipitates and spheroidization of cementites are mainly controlled by the combined effects of high temperature and load stress.

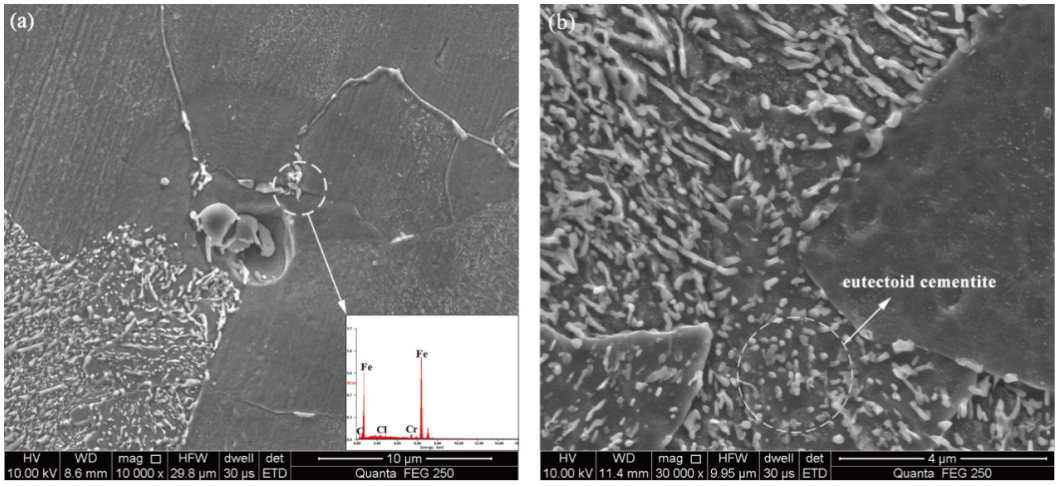

Fig. 7. Microstructure of the (a) precipitates; (b) eutectoid cementites in molten NaCl-70%KCl under the stress of 150MPa.

4. Conclusions

The compression creep deformation behavior and microstructure change of 12Cr1MoV low alloy steel in different molten alkali salts at 650℃ with load stress of 150MPa were investigated in this study. Main conclusions were drawn as follows:

(1) Creep occurred in different molten alkali salts and molten chlorides were proved to accelerate the creep than sulfates. With the increase contents of KCl in molten chloride mixtures, the steady creep rates increase.

(2) On the surfaces, the corrosion was aggravated with the increase of KCl. While unconspicuous holes and cracks were observed on the sample in NaCl-40%Na_2SO_4 because molten sulfates can suppress corrosion effects of chlorides.

(3) On the cross sections, the applied stress plays a synergic role with corrosion leading to the progressive loss of material load-bearing capacity. Obvious cracks were resulted by molten chlorides and load stress. With the increase of KCl, numbers of cracks increase and holes with large size also appeared. Stress concentration easily happened on those defected structures, leading to the deformation of samples.

(4) On the substrates, there is a clear difference on the compression degree of grains in different molten salts. But the corrosion hardly affects the morphology of precipitates and cementites, which is mainly decided by the high temperature and load stress. Both of the tertiary cementites on grain boundaries and spheroidization of cementites decreased a greater driving force and strength of 12Cr1MoV.

Acknowledgement

This work was supported by the National Natural Science Foundation of China (51275058) and College Innovation Platform Project of Hunan Province (13K052)

References

[1] Z.Q. Li, J.M. Han, W.J. Li, L. Pan, Low cycle fatigue behavior of Cr–Mo–V low alloy steel used for railway brake discs, Mater. Des. 56(2014): 146-157.

[2] B.N. Rao, A.R. Acharya, Fracture behavior of a high strength medium carbon low alloy steel, Eng. Fract. Mech. 53(1996): 303-308.

[3] N. Harada, M. Takuma, M. Tsujikawa, K. Higashi, Effects of V addition on improvement of heat shock resistance and wear resistance of Ni–Cr–Mo cast steel brake disc, Wear. 302(2013): 1444–1452.

[4] C.C. Tsaur, J.C. Rock, C.J. Wang, Y.H. Su,The hot corrosion of 310 stainless steel with pre-coated $NaCl/Na_2SO_4$ mixtures at 750°C, Mater. Chem. Phys. 89(2005): 445-453.

[5] R. Saidur, E.A. Abdelaziz, A. Demirbas, M.S. Hossain, S. Mekhilef, A review on biomass as a fuel for boilers, Renew. Sust. Energ. Rev. 15(2011): 2262-2289.

[6] C. Yin, L. A. Rosendahl, Grate-firing of biomass for heat and power production." Prog. Energ. Combust. 34(2008): 725-754.

[7] T. Gruber, K. Schulze, R. Scharler, I. Obernberger, Investigation of the corrosion behaviour of 13CrMo4–5 for biomass fired boilers with coupled online corrosion and deposit probe measurements, Fuel, 144(2015): 15-24.

[8] R.A. Antunes and M.C.L. de Oliveira , Corrosion in biomass combustion: A materials selection analysis and its interaction with corrosion mechanisms and mitigation strategies, Corros. Sci. 76(2013): 6-26.

[9] Z.Q. Lv, B. Wang, Z.H. Wang, S.H. Sun, W.T. Fu, Effect of cyclic heat treatments on spheroidizing behavior of cementite in high carbon steel, Mat. Sci. Eng: A. 574(2013): 143-148.

[10] C.S. Zheng, L.F. Li, W.Y. Yang, Z.Q. Sun,Enhancement of mechanical properties by changing microstructure in the eutectoid steel, Mat. Sci. Eng: A. 558(2012): 158-161.

[11] Y. Xiong, T.T. He, Z.Q. Guo, H.Y. He, F.Z. Ren, A.A. Volinsky, Mechanical properties and fracture characteristics of high carbon steel after equal channel angular pressing, Mat. Sci. Eng: A. 563(2013): 163-167.

[12] J. Ahmad, J. Purbolaksono, L.C. Beng, Thermal fatigue and corrosion fatigue in heat recovery area wall side tubes, Eng. Fail. Anal. 17(2010): 334-343.

[13] S.C.V. Lith, Lab-scale investigation of deposit-induced chlorine corrosion of super heater materials under simulated biomass-firing conditions. Part1:exposure at 560 ℃." Energy Fuels. 23(2009): 3457–3468.

[14] S. Liu, Z.D. Liu, Y.T. Wang, J. Tang,A comparative study on the high temperature corrosion of TP347H stainless steel, C22 alloy and laser-cladding C22 coating in molten chloride salts, Corros. Sci. 83(2014): 396-408.

[15] Role of chlorides in hot corrosion of a cast Fe–Cr–Ni alloy. Part I: Experimental studies."Corros. Sci. 46(2004): 2893-2907.

[16] D.A. Shores, B.P. Mohanty, Role of chlorides in hot corrosion of a cast Fe–Cr–Ni alloy. Part II: thermochemical model studies. Corros. Sci. 46(2004): 2909-2924.

[17] H. Dieringa, N. Hort, K.U. Kainer, Investigation of minimum creep rates and stress exponents calculated from tensile and compressive creep data of magnesium alloy AE42, Mat. Sci. Eng: A. 510-511(2009): 382-386.

[18] M.E. Mehtedi, S. Spigarelli, E. Evangelista, G. Rosen, Creep behaviour of the ZM21 wrought magnesium alloy, Mat. Sci. Eng: A. 510-511(2009): 403-406.

[19] J.D. DeFouw, D.C. Dunand,Processing and compressive creep of cast replicated IN792 Ni-base superalloy foams. Mat. Sci. Eng: A. 558(2012): 129-133.

[20] O. Prat, J. Garcia, D. Rojas, G. Sauthoff, G. Inden, The role of Laves phase on microstructure evolution and creep strength of novel 9%Cr heat resistant steels." Intermetallics. 32(2013): 362-372.

[21] D.L. Lin, W. Huang, Y.H. Zhang, Creep rupture behaviour of salt-coated superalloy GH37 in a hot environment, Acta. Metall. Sin. 23(1987): 413-420.

[22] S. Bagui, A.K. Ray, J.K. Sahu, N. Parida, J. Swaminathan, M. Tamilselvi, S.L. Mannan, Influence of saline environment on creep rupture life of Nimonic-263 for marine turbine application, Mat. Sci. Eng: A. 566(2013): 54-60.

[23] Y.H. Zhang, Creep and fracture of superalloys in hot corrosion environments, Corros.Sci. Prot. Technol. 7(1995): 108-114.

[24] H.J. Grabke, E. Reese, M. Spiegel,The effects of chlorides, hydrogen chloride and sulfur dioxide in the oxidation of steels below deposits, Corros. (1995): 37: 1023–1043.

[25] S.A. Shipilov, Mechanisms for corrosion fatigue crack propagation, Fatigue. Fract. Eng. M. 25(2002): 83-88.

[26] H.L. Yi, Z.Y. Hou, Y.B. Xu, D. Wu, G.D. Wang, Acceleration of spheroidization in eutectoid steels by the addition of aluminum." Scripta. Mater. 67(2012): 645-648.